Antiferromagnetic layer thickness dependence of the magnetization reversal in the epitaxial MnPd/Fe exchange bias system

Qing-feng Zhan,* Wei Zhang, and Kannan M. Krishnan†
Department of Materials Science, University of Washington, Seattle, Washington 98195, USA
(Received 11 September 2010; revised manuscript received 10 January 2011; published 7 March 2011)

We report an investigation on the antiferromagnetic layer thickness dependence of magnetization reversal in *c*-axis oriented MnPd/Fe epitaxial exchange biased bilayers. Several kinds of multistep loops were observed for different samples measured at various field orientation. The evolution of the angular dependent magnetic behavior evolving from a representative Fe film to the exchange biased bilayers was revealed. With increase of the thickness of the antiferromagnetic layers, asymmetrically shaped loops and biased two-step loops are induced by exchange bias. Including the unidirectional anisotropy, a model based on the domain nucleation and propagation was developed, which can nicely describe the evolution of the magnetic behaviors for MnPd/Fe bilayers and correctly predicts the critical angles separating the occurrence of different magnetic switching processes. For fields applied along the bias direction, the 180° magnetic reversal changes from two successive 90° domain wall nucleations to a single 180° domain wall nucleation at the critical thickness of the MnPd layer.

DOI: 10.1103/PhysRevB.83.094404 PACS number(s): 75.70.Cn, 75.60.Jk, 75.30.Gw

I. INTRODUCTION

Exchange bias (EB) was first discovered in Co particles embedded in their native antiferromagnetic oxide by Meiklejohn and Bean.[1] Since then this effect has been found in numerous antiferromagnet(AFM)/ferromagnet(FM) systems, both in particles as well as in layered thin film structures.[2,3] From a scientific point of view, both the properties and the structures for the layered system can be very effectively tuned and characterized.[2,3] From an application point of view, most of the devices based on EB, such as magnetoresistive sensors and magnetic random access memory devices,[4,5] are in thin film form. Consequently, AFM/FM EB bilayers have been widely studied during the past decades.

Due to the exchange coupling at the AFM/FM interface, EB results in a shift of the hysteresis loop H_{eb} in either the positive[6] or the negative[7] field direction and an enhancement of the coercivity H_c.[8] For a bilayer with the given AFM and FM materials, the value of H_{eb} intrinsically depends on the thicknesses of both AFM and FM layers.[2] Previous studies on polycrystalline AFM/FM bilayers have shown that H_{eb} is roughly inversely proportional to the thickness of FM layer t_{FM}, following a phenomenological expression of $H_{eb} = \Delta\sigma/M_{FM}t_{FM}$, where $\Delta\sigma$ is the exchange coupling energy per unit area and M_{FM} is the saturation magnetization of the FM layer.[9] This relation reveals that EB originates at the AFM/FM interface. In contrast, the dependence of H_{eb} on the AFM thickness t_{AFM} is more complicated.[9] Ali *et al.*, performed a systematical investigation on the t_{AFM} dependence of EB in IrMn/Co at various temperatures.[10] At low temperatures, as t_{AFM} increases, H_{eb} sets in at very low t_{AFM} and then appears as a sharp peak before finally decaying to a constant value, while at high temperature, the critical t_{AFM} increases and the peak of H_{eb} moves to higher t_{AFM} and gradually disappears.[10]

Compared to the extensive investigation on polycrystalline EB systems, there are only a few works focused on epitaxial films.[11,12] Thanks to the clear AFM/FM interface and the well-controlled magnetic configuration near the AFM/FM interface, the epitaxial exchange biased bilayers are regarded as ideal systems for investigating the underlying physics of exchange bias and have attracted much attention in recent years.[13] Our work on epitaxial MnPd/Fe bilayers has shown that H_{eb} holds the same $1/t_{FM}$ dependence on the FM layer.[14] However, the dependence of EB on t_{AFM} for the epitaxial EB systems including MnPd/Fe is not well known.

Magnetic anisotropy is one of the fundamental physical parameters which determine the magnetization reversal processes in magnetic films.[15] For AFM/FM bilayers, a unidirectional anisotropy K_{eb} is established by EB and accompanied by an induced uniaxial anisotropy K_u, which plays the key role in altering the magnetic switching process and often results in the asymmetric reversal processes, i.e., domain nucleation and propagation for one field branch and moment rotation for the opposite field branch.[16,17] Considering both K_{eb} and K_u, the value of EB and coercivity for the polycrystalline EB systems can be numerically fitted by the Stoner-Wohlfarth model.[18] In epitaxial EB systems the intrinsic magnetocrystalline anisotropy, which results in multistep hysteresis loops and a complex angular dependent behavior,[11,12,14] needs to be further considered. An effective field model, which considers the contributions to the effective field acting on the FM layer during magnetization reversal, was developed by Arenholz *et al.*, to quantitatively interpret the complicated angular dependent switching fields.[12] On the other hand, both the multistep loops and the angular dependent behaviors for the epitaxial Fe single layers can be described by a model based on domain wall (DW) nucleation.[19,20] Up till now, the evolution of magnetic reversal on t_{AFM}, especially for the epitaxial systems, from the FM single layer ($t_{AFM} = 0$) to the AFM/FM bilayers has not been well understood.

In this paper, we present a study on the dependence of EB on the AFM thicknesses for the epitaxial MnPd/Fe bilayers. Different magnetic switching processes were observed at various field orientations. With increasing thickness of the MnPd layer, the angular dependent magnetic behavior was found to evolve from the type of the FM single layer to that of AFM/FM EB bilayers, which can be explained by a model based on domain nucleation.

II. EXPERIMENT

C-axis oriented MnPd/Fe bilayers were epitaxially grown on optically transparent MgO(001) substrates, according to the relationships MnPd(001)‖Fe(001)‖MgO(001) and MnPd[100]‖Fe[110]‖MgO[100], at a temperature of 310 °C in an ion beam sputtering system. The thickness of the Fe layer was fixed at 10 nm and the thickness of the MnPd layer, t_{MnPd}, was varied from 0 to 75 nm. An external magnetic field of 300 Oe along the Fe[010] direction was applied during growth. Samples were protected from oxidation by a 4 nm thick Ta layer. Magnetic characterization was performed *ex situ* at room temperature by using a combined longitudinal and transverse magneto-optics Kerr effect (MOKE) setup and by illuminating the samples from the bottom side through the transparent substrates. The magnetic field is applied parallel and normal to the plane of incidence of the laser beam for the longitudinal and the transverse MOKE geometries, respectively. Meanwhile, the field orientation is restricted in the film surface, but can take an arbitrary angle with respect to the in-plane crystal direction for the both configurations. Such a combined MOKE setup is sensitive to both the longitudinal and the transverse Kerr rotation and enables us to measure the components of the in-plane magnetization vector both parallel and perpendicular to the magnetic field during the magnetization reversal.[21] More details on the experiment are described elsewhere.[14,22,23]

III. EXPERIMENTAL RESULTS AND DISCUSSION

Figure 1 summarizes the anisotropy geometry and the magnetic switching routes used in this paper. The exchange bias gives rise to a unidirectional anisotropy K_{eb} and a collinear uniaxial anisotropy K_u along the field-cooling direction.[14] Both of them are superimposed on the Fe cubic magnetocrystalline anisotropy K_1, thus inducing various magnetic switching routes between the Fe easy axes for the external field H applied along different orientations ϕ,[11,14] as defined for the angle between H and the bias direction. Depending on the initial and the final remanent directions involved in the magnetic transition, we refer to the corresponding switching fields as H_{c1} to H_{c4} and $H_{c\mathrm{I}}$ to $H_{c\mathrm{IV}}$, respectively. For the switching from the $[0\bar{1}0]$ to [010] axes, the critical field is H_c.

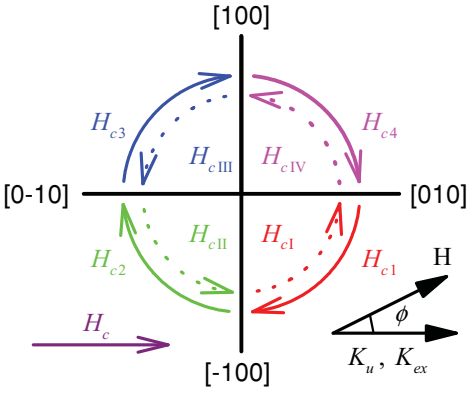

FIG. 1. (Color online) The anisotropy geometry for the epitaxial MnPd/Fe exchanged biased bilayers. Fe cubic anisotropy is superimposed on the EB-induced unidirectional and uniaxial anisotropies aligned along the Fe[010] axis. The coercivities for the magnetic switching between different Fe easy axes are defined. The external field is applied at an angle ϕ with respect to the bias direction.

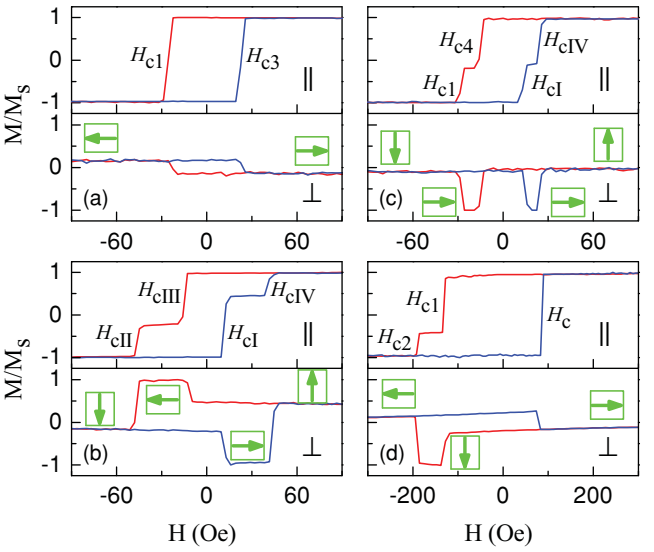

FIG. 2. (Color online) Typical longitudinal (‖) and transverse (⊥) MOKE loops measured at various field orientation. (a) Square loop, (b) unbiased two-step loop, and (c) biased two-step loop are obtained at $\phi = 0°$, 65°, and 90°, respectively, for MnPd/Fe film with $t_{\mathrm{MnPd}} =$ 10 nm. With increasing AFM thickness, (d) an asymmetrically shaped loop is observed, such as for the bilayer with $t_{\mathrm{MnPd}} = 75$ nm measured at $\phi = 20°$. The red and the blue curves correspond to the descending and the ascending branches of the hysteresis loops, respectively. The orientation of Fe spins in the switching processes is represented by the arrows enclosed in the square. The coercivities based on the magnetic switching routes are presented as well.

Both longitudinal (‖) and transverse (⊥) loops were obtained for ϕ varied from −45° to 135° in steps of 5°. Four typical kinds of multistep hysteresis loops are observed in various samples, as depicted in Fig. 2. The Fe spin orientations in each step and the coercivities based on the switching paths are presented as well. The square loops are obtained for ϕ around the bias direction, and the corresponding transverse MOKE signal indicates the magnetization switches between the [010] and $[0\bar{1}0]$ axes via DW nucleation and propagation [Fig. 2(a)]. When the field orientation is farther away from the bias direction, one can observe the two-step switching process with the intermediate states in which Fe spins are oriented perpendicular to the initial and final remanent axes. The transverse MOKE loops show that the intermediate states for the ascending and descending branches can lie on the two opposite Fe easy axes [Fig. 2(b)] or on the same axis given by the bias, i.e., the [010] direction [Fig. 2(c)].

Similar to Fe/MgO(001) films that we previously produced by using molecular beam epitaxy (MBE),[24] the present Fe single layer grown by IBS, i.e., $t_{\mathrm{MnPd}} = 0$, exhibits the square and the double-side two-step loops for ϕ close to 0° and 90°, respectively, due to a weak uniaxial anisotropy superimposed on Fe cubic anisotropy. Without the AFM layer, all the hysteresis loops of the Fe layer are symmetrical with respect to the central point ($H = 0$ and $M = 0$), while the angular dependence of the switching fields has a symmetry about both

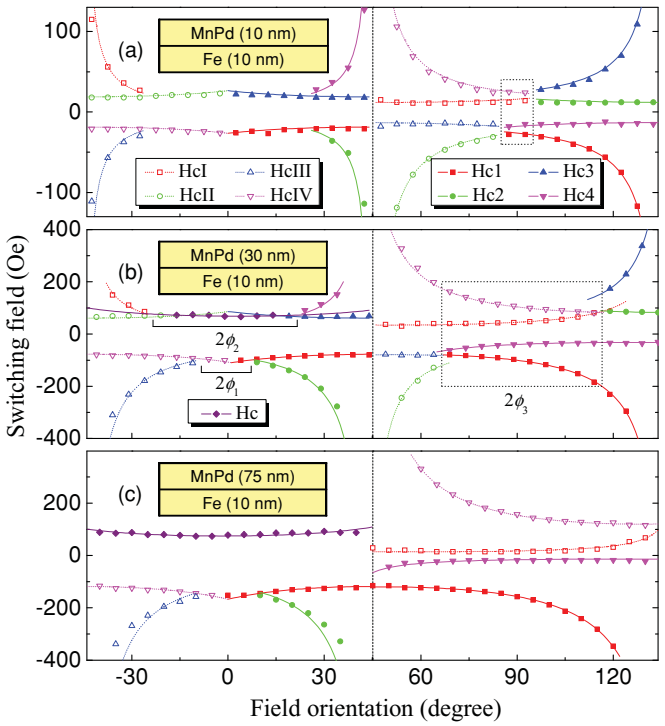

FIG. 3. (Color online) Typical field orientation dependence of the experimentally observed switching fields (symbols) and the corresponding theoretical fitting results (curves) for MnPd/Fe bilayers with (a) $t_{\mathrm{MnPd}} = 10$ nm, (b) $t_{\mathrm{MnPd}} = 30$ nm, and (c) $t_{\mathrm{MnPd}} = 75$ nm. The switching fields represented by the different symbols and curves correspond to the magnetic transitions between different initial and final Fe easy axes. The 180° magnetic transition occurs in the range of $-\phi_1 < \phi < \phi_1$ for the descending branch and $-\phi_2 < \phi < \phi_2$ for the ascending branch, respectively. The biased two-step magnetic switching process takes place in the range of $90° - \phi_3 < \phi < 90° + \phi_3$, as enclosed in a dashed square.

$H = 0$ and the Fe easy directions. After depositing an AFM layer on top of the Fe layer, these loops are shifted H_{eb} in the negative field direction due to the AFM/FM interfacial exchange coupling. Moreover, the one-side two-step switching event appears for the field perpendicular to the bias direction. From this we can infer that the [010] direction is the combined easy axis of the cubic, uniaxial, and unidirectional anisotropies. In the case where ϕ is close to 90°, the magnetic switching processes for both branches are mediated via this same Fe easy axis, which is more energetically favorable, rather than the opposite one. Figure 3(a) presents the ϕ dependence of the switching fields for $t_{\mathrm{MnPd}} = 10$ nm. The square and the biased two-step switching events occur for $-25° < \phi < 25°$ and $85° < \phi < 95°$, respectively. Because H_{eb} for the bilayers with $t_{\mathrm{MnPd}} \leqslant 10$ nm is very weak (less than 5 Oe), their angular dependent behaviors still look symmetrical about $H = 0, \phi = 0°$ and 90°, as for the Fe/MgO(001) films.[24]

With further increasing t_{MnPd} to 20 and 30 nm, the bilayers show a clear H_{eb}. Moreover, asymmetrically shaped hysteresis loops are observed with two-step magnetic transition for the descending branch and one-step for the ascending branch, as revealed in Fig. 2(d). This type of loop appears between the regimes where the square and the two-step loops occur. Consequently, it can be seen in the ϕ dependence of switching fields for $t_{\mathrm{MnPd}} = 30$ nm shown in Fig. 3(b) that the range of angle for which the 180° magnetic transition occurs becomes different for the two branches of the loops. The critical angle ϕ_1 separating the occurrence of one-step and two-step magnetic switching processes for the descending branch is ∼7°, and the other critical value ϕ_2 for the ascending branch is ∼23° [see Fig. 3(b)]. As compared to the sample with $t_{\mathrm{MnPd}} = 10$ nm, ϕ_1 is clearly reduced due to the enhancement of EB, but ϕ_2 remains similar. Meanwhile, the biased two-step regime ϕ_3, as indicated by the dashed square in Fig. 3, is expanded to 25°. The ϕ-dependent switching fields reveal the obvious asymmetry about $\phi = 90°$, which indicates that the anisotropy symmetry about $\phi = 90°$ is significantly broken by the pronounced K_{eb}.

For bilayers with thicker t_{MnPd} at 45 and 75 nm, H_{eb} keeps increasing and the angular dependent behavior evolves to the type shown in Fig. 3(c). The 180° magnetic transition takes place in the whole range of angles from −45° to 45° for the ascending branch, the critical angle $\phi_2 = 7°$ remains unchanged as compared to that for $t_{\mathrm{MnPd}} = 30$ nm, and the biased two-step loops are obtained for $45° < \phi < 135°$, i.e., $\phi_3 = 45°$. It should be noted that ϕ_3 is not monotonously enhanced with increasing t_{MnPd}, especially when t_{MnPd} is thin, which will be discussed below.

Since we study the AFM thickness dependence of magnetic properties, an inevitable question is what the critical t_{MnPd} is for the onset of EB. Ali *et al.*, have reported that a thickness of 2.1 nm IrMn is needed to produce an exchange bias in a polycrystalline system.[10] In our experiment, both the measurement step of the field and the remanence of the electromagnet are around 2 Oe. Therefore, it is hard to say if a loop shift of ∼2 Oe is the result of the exchange bias or measurement error. We have shown above that EB leads to the occurrence of the one-side two-step magnetic transition [see Fig. 2(c)]. Consequently, the observation of the one-side transverse MOKE loop can be viewed as the criteria to estimate the minimum t_{MnPd} which can induce exchange bias. For the samples with $t_{\mathrm{MnPd}} = 5$, 2, and 1 nm, the regime for observing the biased two-step loops is $\phi_3 = 17°, 10°$, and 3°, respectively. Assuming the loops measured at $\phi = 90°$ are symmetric about $H = 0$, we can minimize the measurement error for the loops obtained at $\phi = 0°$ and get $H_{\mathrm{eb}} = 2.5$ Oe for $t_{\mathrm{MnPd}} = 1$ nm. That is to say, the critical thickness of the AFM layer establishing the exchange bias in our system is even below 1 nm. Below this thickness, it is difficult for the parallel AFM DW to exist.[25] In any case, our experiment provides a new way to determine this critical AFM thickness with great accuracy.

IV. MAGNETIZATION REVERSAL MECHANISM

Now we turn to the ϕ dependence of switching fields. Considering a weak K_u parallel to the [010] axis, we have previously shown that both the one-step and the two-step loops observed in epitaxial Fe/MgO(001) films are mediated by two successive or two separate 90° DW nucleations.[20,24] The strength of K_u and the DW nucleation energy $\varepsilon_{90°}$ can be evaluated by fitting the ϕ dependence of switching fields. For the MnPd/Fe system, the AFM layer induces an additional

anisotropy term, i.e., $K_{\rm eb}$, and enhances K_u. As a result, the total energy for the Fe bilayer can be rewritten as

$$E = \frac{K_1}{4}\sin^2 2\theta - K_u\cos^2\theta - K_{\rm eb}\cos\theta - MH\cos(\phi-\theta),$$

where θ is the angle between the magnetization M and the bias direction. Theoretically, both the coherent rotation and the DW nucleation can result in irreversible Barkhausen jumps; the two reversal mechanisms as well as the asymmetrical one have been observed in various EB systems.[17,18,26,27] We have tried to use the coherent rotation to explain the hysteresis loops for a-axis oriented MnPd/Fe EB bilayers, but the prediction for the coercivity is obviously too large.[28] On the other hand, by using Lorentz transmission electron microscopy, Wang *et al.* directly observed that the magnetization reversal in epitaxial IrMn/Fe bilayers occurs through DW nucleation and propagation.[26] Inspired by these works, we tentatively extend the DW nucleation model developed for Fe/MgO(001) films to account for the magnetization reversal in epitaxial MnPd/Fe EB bilayers. The energies of single domain states at these four Fe easy axes are

$$\begin{aligned} E_{[010]} &= -K_{\rm eb} - K_u - MH\cos\phi, \\ E_{[100]} &= -MH\sin\phi, \\ E_{[0\bar{1}0]} &= K_{\rm eb} - K_u + MH\cos\phi, \\ E_{[\bar{1}00]} &= MH\sin\phi. \end{aligned}$$

The switching fields related to the DW nucleation energy can be derived from the energy gain between the local minima at the initial and final easy axes involved in the transition.[19,29] The theoretical switching fields for 90° magnetic transitions, as indicated in Fig. 1, are obtained as

$$\begin{aligned} H_{c1} &= \frac{\varepsilon_{90^\circ} + K_{\rm eb} + K_u}{M(-\sin\phi - \cos\phi)}, \quad H_{c2} = \frac{\varepsilon_{90^\circ} + K_{\rm eb} - K_u}{M(\sin\phi - \cos\phi)}, \\ H_{c3} &= \frac{\varepsilon_{90^\circ} - K_{\rm eb} + K_u}{M(\sin\phi + \cos\phi)}, \quad H_{c4} = \frac{\varepsilon_{90^\circ} - K_{\rm eb} - K_u}{M(-\sin\phi + \cos\phi)}, \\ H_{c\rm I} &= \frac{\varepsilon_{90^\circ} - K_{\rm eb} - K_u}{M(\sin\phi + \cos\phi)}, \quad H_{c\rm II} = \frac{\varepsilon_{90^\circ} - K_{\rm eb} + K_u}{M(-\sin\phi + \cos\phi)}, \\ H_{c\rm III} &= \frac{\varepsilon_{90^\circ} + K_{\rm eb} - K_u}{M(-\sin\phi - \cos\phi)}, \quad H_{c\rm IV} = \frac{\varepsilon_{90^\circ} + K_{\rm eb} + K_u}{M(\sin\phi - \cos\phi)}. \end{aligned}$$

For 180° magnetic switching from the $[0\bar{1}0]$ to [010] axes,

$$H_c = \frac{\varepsilon_{180^\circ} - 2K_{\rm eb}}{2M(\cos\phi)},$$

where ε_{180° is 180° DW nucleation energy. To our surprise, we find that if ε_{90°/M is replaced by the anisotropy field, our theoretical expressions based on the DW nucleation are exactly the same as the equations derived from the effective field model.[12] In that model, comparing the effective fields at different Fe easy axes involved in a magnetic transition, the authors were able to interpret the angular dependence of the switching fields, although they did not specify if the magnetization reversal mechanism is coherent rotation or DW nucleation.

Certainly, the ϕ dependence of switching fields for an Fe single layer, i.e., $t_{\rm MnPd} = 0$, can be nicely fitted[24] by the DW nucleation model with $\varepsilon_{90^\circ}/M = 5.0$ Oe, $K_u/M = 2.4$ Oe, and $K_{\rm eb}/M = 0$ Oe. It should be noted that according to the reversal mechanism caused by two successive 90° DW nucleations, the switching fields for the square loops are fitted by H_{c1} and H_{c3}, but not H_c derived from the 180° DW nucleation.[20] This is why we mark H_{c1} and H_{c3} as the switching fields for the square loop shown in Fig. 2(a). The critical angles separating the occurrence of different switching routes can be predicted by comparing the switching fields given by different possible routes. In the case of $0^\circ < \phi < 45^\circ$, the switching process for the descending branch is determined by the relationship between H_{c1} and H_{c2}, while for the ascending branch by the comparison of H_{c3} and H_{c4}. The one-step and two-step routes correspond to $H_{c1} < H_{c2}$ ($H_{c3} > H_{c4}$) and $H_{c1} > H_{c2}$ ($H_{c3} < H_{c4}$) for deceasing (increasing) field, respectively. Consequently, one can obtain $\phi_1 = \arctan[K_u/(\varepsilon_{90^\circ} + K_{\rm eb})]$ and $\phi_2 = \arctan[K_u/(\varepsilon_{90^\circ} - K_{\rm eb})]$. Obviously, for an EB sample with $K_{\rm eb}$, $\phi_1 < \phi_2$, which leads to the observation of the asymmetrically shaped loops for $\phi_1 < \phi < \phi_2$. When $45^\circ < \phi < 90^\circ$, whether the magnetization switching from [100] clockwise to [010] or counterclockwise to $[0\bar{1}0]$ depends on which path gives the lower coercivity. Thus, comparison of $H_{c\rm III}$ and H_{c4} yields $\phi_3 = \operatorname{arccot}[(\varepsilon_{90^\circ} - K_u)/K_{\rm eb}]$. For the special case of Fe film in which $K_{\rm eb} = 0$, $\phi_3 = 0$, that is, no biased two-step loops can be observed. Moreover, $\phi_2 = \phi_3 = \arctan(K_u/\varepsilon_{90^\circ})$. This is exactly the conclusion in Ref. 20.

Using the above-derived model based on DW nucleation, we successfully fit all the ϕ dependence of switching field. The corresponding theoretical curves are illustrated in Fig. 3. The only remaining problem is to fit the coercivities for the 180° magnetic switching from the $[0\bar{1}0]$ to [010] axes, which takes place for the ascending branch around the bias direction. When $t_{\rm MnPd} \leqslant 10$ nm, the ϕ-dependent switching field reveals a peak at $\phi = 0^\circ$ [see Fig. 4(a) for a detailed view], which can be described by using the magnetization reversal mechanism of two successive 90° DW nucleations developed for Fe/MgO(001) films.[20] However, for $t_{\rm MnPd} \geqslant 45$ nm, as shown Fig. 4(b), the ϕ dependence of the experimental data shows no longer a peak but a minima at the bias direction, which can be fitted by the theoretical equation of H_c as derived above according to the mechanism of 180° DW nucleation. For 10 nm$< t_{\rm MnPd} <$ 45 nm, neither of the two mechanisms can very well describe this angular dependent behavior, as shown in Fig. 3(b). The experimental results imply that EB leads to an evolution in the reversal mechanism for the 180° magnetic switching from the $[0\bar{1}0]$ to [010] axes. When the AFM thickness is thin and $H_{\rm eb}$ is very weak, the reversal mechanism of MnPd/Fe bilayers is much closer to the two successive 90° DW nucleations observed in the Fe single layer, but increasing $t_{\rm MnPd}$, that is, exerting a rather strong $K_{\rm eb}$ on the Fe layer, changes the switching behavior to 180° DW nucleation. It should be noted that although the behavior of the ϕ dependence of 180° magnetic switching fields for the ascending branch occurring near $\phi = 0^\circ$ changes with increasing $t_{\rm MnPd}$, it is not the same for the descending branch in which the ϕ-dependent switching fields continuously can be fitted by the model of two successive 90° DW nucleations for all MnPd/Fe samples with different $t_{\rm AFM}$ as well as different $t_{\rm FM}$.[14] Similar phenomena have also been observed in epitaxial IrMn/Fe EB bilayers with various thicknesses of the IrMn layer.[30]

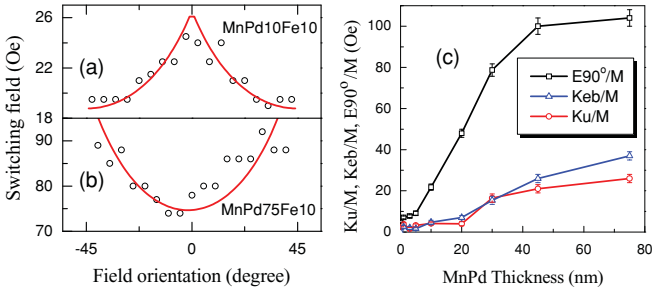

FIG. 4. (Color online) The detailed view of the angular dependence of the switching fields (a) $H_{c\mathrm{II}}$ and H_{c3} for the MnPd/Fe bilayer with $t_{\mathrm{MnPd}} = 10$ nm and (b) H_c for the sample with $t_{\mathrm{MnPd}} = 75$ nm. They can be interpreted by the magnetic reversal mechanism of two successive 90° DW nucleations and a 180° DW nucleation, respectively. (c) The parameters ε_{90°/M, K_{eb}/M, and K_u/M given by the fitting for the angular dependence of switching fields for MnPd/Fe bilayers with different t_{MnPd}.

In Fig. 4(c), we plot the parameters ε_{90°/M, K_{eb}/M, and K_u/M generated from the fitting for MnPd/Fe bilayers with different t_{MnPd}. K_{eb}/M can be directly linked to H_{eb}.[16] The DW nucleation energy has the relationship of $\varepsilon_{180^\circ}/2 = \varepsilon_{90^\circ} + K_{\mathrm{eb}}$, since the difference between the left and the right switching fields for the square loops at $\phi = 0^\circ$ is defined as $2H_{\mathrm{eb}}$, i.e., $2K_{\mathrm{eb}}/M$. Using the fitting parameters, one can theoretically obtain the asymmetrical range of angles of ϕ_1 and ϕ_2, as well as the critical angle ϕ_3 for the biased two-step magnetic switching; they are in good agreement with the experimental observation. H_{eb} for c-axis MnPd/Fe samples is enhanced with increasing t_{MnPd}, but does not reach saturation even for our thickest sample at $t_{\mathrm{MnPd}} = 75$ nm, which differs from our previous a-axis oriented MnPd/Fe samples and other systems.[2,28] K_u shows a similar trend as K_{eb}, because EB also induces a uniaxial anisotropy. However, when $t_{\mathrm{MnPd}} \leqslant 5$ nm, the contribution of EB on inducing K_u is as weak as that from other origins, e.g., the atomic steps on the substrates and the defects of the films. These other contributions not from EB depend mostly on the detailed experimental process and the surface of the substrates; thus they are quite random and not very controllable.[24] Because of the sample-to-sample variation, K_u is not strictly increased with increasing t_{MnPd} for $t_{\mathrm{MnPd}} \leqslant 5$ nm, which therefore causes the critical angle ϕ_3 not to monotonically increase with enhancement of t_{MnPd}, as we mentioned above. The increasing DW nucleation energy can be understood considering the interfacial states including the roughness, the interdiffusion, the dislocations, and the rotatable Mn moments at the AFM/FM interface. All these factors can be varied with the thicknesses of both the Fe and MnPd layers. The x-ray reflectivity curves (not shown) for the series of MnPd/Fe bilayers exhibit good oscillation, which qualitatively indicates that the interfaces in the samples with various t_{MnPd} are quite sharp; both the interdiffusion and the roughness are rather low. However, the lattice mismatch between MnPd and Fe layers results in the crystal lattice distortion and the strain in the films, which gives rise to the magnetoelastic anisotropy. With increasing t_{MnPd}, the strain is relaxed via the formation of dislocations at the interface.[24,28] These dislocations, the interfacial roughness, and the diffusing atoms can act as the pinning centers for DW nucleation and therefore enhance the nucleation energy. On the other hand, near the interface, there are some rotatable Mn spins which are strongly coupled with Fe moments and which may follow the motion of the Fe layer.[31] These moments cannot result in the exchange bias, but instead increase the coercivity;[31,32] this is reflected in the magnitude of the DW nucleation energy according to our model. The increase of H_{eb}, but below saturation even at $t_{\mathrm{MnPd}} = 75$ nm, also can be explained by the presence of various interfacial defects. The existence of the defects near the interface leads to the formation of domains in AFM layers.[25,33] The increase of t_{MnPd} results in the increase of dislocations in the AFM layers. Therefore, the corresponding AFM domain size will be reduced, which causes the increase of EB.[34] However, the amount of the defects resulting from the strain relaxation is quite limited, so for bilayers in which both AFM and FM layers are epitaxially grown on the substrates, it is hard for EB to reach saturation. In contrast, the polycrystalline EB systems can achieve the maximum H_{eb} in rather thin AFM layers.[2,10] Furthermore, the other interfacial defects of the roughness, the interdiffusion, and the rotatable Mn moments make greater or lesser contributions to the increase of EB. Therefore, in order to enhance our understanding of the AFM thickness dependence of EB in the epitaxial MnPd/Fe system, it would be helpful to further determine the exact status of the interface and their changes with varying t_{MnPd}. Additional characterizations by using x-ray resonant magnetic reflectometry (XRMR) and high resolution transmission electron microscopy (HRTEM) to measure the interfaces or the cross sections are in progress.

V. CONCLUSIONS

In summary, we have fabricated c-axis oriented MnPd/Fe bilayers in which both the antiferromagnetic and the ferromagnetic layers are epitaxially grown on MgO(001) substrates at a well-controlled temperature. The magnetic properties for the samples with different thicknesses of the MnPd layer were characterized by using combined longitudinal and transverse magneto-optical Kerr effects. Square loops, asymmetrically shaped loops, and both biased and unbiased types of two-step loops were observed for measurements at various field orientations. The onset of biased two-step loops is shown to be a good estimate of the minimum AFM thickness required for establishing exchange bias; for our MnPd/Fe system, the value was found to be even below 1 nm. The process for the angular dependence of switching fields evolving from the typical behavior of the single Fe film to that of the exchange biased bilayer was revealed. With the increase of t_{MnPd}, asymmetrical and biased two-step loops are induced because the anisotropy symmetry of Fe is broken by the EB induced unidirectional anisotropy. Considering the cubic, the uniaxial, and the unidirectional anisotropies, we developed a model based on domain nucleation to interpret the evolution process for the angular dependent behavior of the series of MnPd/Fe bilayers, and predict the range of angle where the different magnetic switching processes occur. From the fitting for the experimental switching fields, we found that the magnetization

reversal mechanism for the 180° magnetic transition occurring near the bias direction changes from two successive 90° DW nucleations to the one-step 180° DW nucleation for one branch, and remains unchanged for the other branch.

ACKNOWLEDGMENTS

This work was supported by the DoE/BES under Grant No. ER45987.

*Present address: Ningbo Institute of Materials Technology and Engineering, Chinese Academy of Sciences, Ningbo, Zhejiang 315201, People's Republic of China.; zhanqf@nimte.ac.cn.
†kannanmk@u.washington.edu

[1] W. H. Meiklejohn and C. P. Bean, Phys. Rev. **102**, 1413 (1956).
[2] J. Nogués and I. K. Schuller, J. Magn. Magn. Mater. **192**, 203 (1999).
[3] J. Nogués, J. Sort, V. Langlais, V. Skumryev, S. Suriñach, J. S. Muñoz, and M. D. Baró, Phys. Rep. **422**, 65 (2005).
[4] S. A. Wolf, D. D. Awschalom, R. A. Buhrman, J. M. Daughton, S. von Molnar, M. L. Roukes, A. Y. Chtchelkanova, and D. M. Treger, Science **294**, 1488 (2001).
[5] C. Chappert, A. Fert, and F. N. V. Dau, Nature Mater. **6**, 813 (2007).
[6] J. Nogués, D. Lederman, T. J. Moran, and Ivan K. Schuller, Phys. Rev. Lett. **76**, 4624 (1996).
[7] J. Nogués, T. J. Moran, D. Lederman, I. K. Schuller, and K. V. Rao, Phys. Rev. B **59**, 6984 (1999).
[8] M. D. Stiles and R. D. McMichael, Phys. Rev. B **63**, 064405 (2001).
[9] R. Jungblut, R. Coehoorn, M. T. Johnson, J. aan de Stegge, and A. Reinders, J. Appl. Phys. **75**, 6659 (1994).
[10] M. Ali, C. H. Marrows, M. Al Jawad, B. J. Hickey, A. Misra, U. Nowak, and K. D. Usadel, Phys. Rev. B **68**, 214420 (2003).
[11] C. H. Lai, Y. H. Wang, C. R. Chang, J. S. Yang, and Y. D. Yao, Phys. Rev. B **64**, 094420 (2001).
[12] E. Arenholz and K. Liu, Appl. Phys. Lett. **87**, 132501 (2005).
[13] A. Mougin, S. Mangin, J. F. Bobo, and A. Loidl, Eur. Phys. J. B **45**, 155 (2005).
[14] Q. F. Zhan and K. M. Krishnan, J. Appl. Phys. **107**, 09D703 (2010).
[15] M. T. Johnson, P. J. H. Bloemen, F. J. A. den Broeder, and J. J. de Vries, Rep. Prog. Phys. **59**, 1409 (1996).
[16] C. Leighton, M. R. Fitzsimmons, P. Yashar, A. Hoffmann, J. Nogués, J. Dura, C. F. Majkrzak, and I. K. Schuller, Phys. Rev. Lett. **86**, 4394 (2001).
[17] P. Blomqvist, K. M. Krishnan, and H. Ohldag, Phys. Rev. Lett. **94**, 107203 (2005).
[18] J. Camarero, J. Sort, A. Hoffmann, J. M. García-Martín, B. Dieny, R. Miranda, and J. Nogués, Phys. Rev. Lett. **95**, 057204 (2005).
[19] R. P. Cowburn, S. J. Gray, J. Ferré, J. A. C. Bland, and J. Miltat, J. Appl. Phys. **78**, 7210 (1995).
[20] Q. F. Zhan, S. Vandezande, K. Temst, and C. Van Haesendonck, Phys. Rev. B **80**, 094416 (2009).
[21] Z. Q. Qiu and S. D. Bader, Rev. Sci. Instrum. **71**, 1243 (2000).
[22] N. Cheng, J. P. Ahn, and K. M. Krishnan, J. Appl. Phys. **89**, 6597 (2001).
[23] P. Blomqvist, K. M. Krishnan, and D. E. McCready, J. Appl. Phys. **95**, 8019 (2004).
[24] Q. F. Zhan, S. Vandezande, K. Temst, and C. Van Haesendonck, New J. Phys. **11**, 063003 (2009).
[25] A. P. Malozemoff, Phys. Rev. B **35**, 3679 (1987).
[26] S. G. Wang, A. Kohn, C. Wang, A. K. Petford-Long, S. Lee, R. Fan, J. P. Goff, L. J. Singh, Z. H. Barber, and R. C. C. Ward, J. Phys. D **42**, 225001 (2009).
[27] S. Brems, K. Temst, and C. Van Haesendonck, Phys. Rev. Lett. **99**, 067201 (2007).
[28] Q. F. Zhan and K. M. Krishnan, Appl. Phys. Lett. **96**, 112506 (2010).
[29] R. P. Cowburn, S. J. Gray, and J. A. C. Bland, Phys. Rev. Lett. **79**, 4018 (1997).
[30] W. Zhang, Q. F. Zhan, and K. M. Krishnan, e-print arXiv:1102.5387v1.
[31] S. Brück, G. Schütz, E. Goering, X. Ji, and K. M. Krishnan, Phys. Rev. Lett. **101**, 126402 (2008).
[32] J. Wu, J. S. Park, W. Kim, E. Arenholz, M. Liberati, A. Scholl, Y. Z. Wu, Chanyong Hwang, and Z. Q. Qiu, Phys. Rev. Lett. **104**, 217204 (2010).
[33] U. Nowak, K. D. Usadel, J. Keller, P. Miltényi, B. Beschoten, and G. Güntherodt, Phys. Rev. B **66**, 014430 (2002).
[34] P. Miltényi, M. Gierlings, J. Keller, B. Beschoten, G. Güntherodt, U. Nowak, and K. D. Usadel, Phys. Rev. Lett. **84**, 4224 (2000).